Available online at www.sciencedirect.com

ScienceDirect

Procedia Computer Science 93 (2016) 176 – 182

Procedia Computer Science

6th International Conference On Advances In Computing & Communications, ICACC 2016, 6-8 September 2016, Cochin, India

Robust Precoded OSTBC For GFDM Systems

Shravan Kumar Bandari[a,*], V.V. Mani[a], A. Drosopoulos[b]

[a]*Department of Electronics and Communication Engineering, National Institute of Technology Warangal, Warangal 506004, India*
[b]*Electrical Engineering, TEI Western Greece, Patras 26334, Greece*

Abstract

Generalized Frequency Division Multiplexing (GFDM) has been proposed recently as a candidate for the next generation wireless communications systems (5G) due to its attractive properties that seem to cover the envisioned applications. In order to make GFDM more robust to multipath fading effects the techniques of space-time block codes (STBC) can be added to its implementation. In this article, we consider the performance of orthogonal space-time block coded (OSTBC) GFDM systems over Rayleigh fading channel. In addition, to further enhance performance, Discrete Prolate Spheroidal Sequences (DPSSs or multi-tapers) can be exploited to turn conventional GFDM to an improved orthogonal system. In this work we investigated a precoded OSTBC Multi-taper GFDM system along with conventional GFDM. The symbol error rate (SER) performance for precoded OSTBC-(M)GFDM systems over a Rayleigh fading channel is examined and a good match between simulation results and analytical expressions is seen to exist.

Peer-review under responsibility of the Organizing Committee of ICACC 2016

Keywords: GFDM; Symbol Error Rate (SER); orthogonal spacetime block code (OSTBC); Rayleigh fading channel.

1. Introduction

With a wide range of envisioned applications like tactile internet, machine to machine (M2M) communication and internet of things (IoT), there is a high demand for one or more new multi-carrier waveform designs in order to serve the never ending wireless needs. Next generation wireless communication systems are not only expected to achieve high data rates of Giga byte connectivity, they are also expected to perform well on high energy efficient networks, be reliable, exhibit low latency in applications, support high density users and use efficiently and with high capacity the available spectrum.

OFDM is currently the most used multicarrier (MC) technique in many standards due to its robustness to multipath fading effects and simple implementation[1]. OFDM uses guard bands to overcome inter-carrier and inter-symbol interference (ICI/ISI), which leads to spectrum under-utilization. This is not a desirable factor in the context of 5G cellular communication systems. In addition, the high out-of-band (OOB) leakage in OFDM makes it challenging and difficult to meet future wireless needs.

* Corresponding author. Tel.: +91-9966285543.
E-mail address: shravnbandari@gmail.com

Peer-review under responsibility of the Organizing Committee of ICACC 2016
doi:10.1016/j.procs.2016.07.198

In order to mitigate the effects of fading, spatial diversity is one of the effective ways to improve performance of wireless communication systems. This can be achieved by employing multiple antennas at either the transmitter side (transmit diversity) and/or the receiver side (receive diversity). In practise, the latter is difficult to implement and most research and development in this area is carried out for the transmit diversity case.

Space-time block coding (STBC), proposed by Alamouti [2] and referred to as an open-loop system, is one of the most well-known transmit diversity schemes to achieve full diversity. The basic idea is simply the transmission of a signal over two independently fading channels. Due to its practical importance, STBC is implemented in third generation networks. In addition, a class of STBC known as Orthogonal space time coding (OSTBC) has been proposed by [3]. This achieves full diversity and at the same time exhibits low decoding complexity at the receiver. In particular, [4,5] deal with OSTBC with partial channel knowledge and a limited feedback system. More recent advancements in precoding techniques have led to precoded OSTBC, which aims to improve overall system performance and maintain full diversity [6,7].

GFDM, proposed as a contender for 5G, is a non-orthogonal block based MC transmission scheme in which each subcarrier is filtered with a circular pulse shaping filter with low OOB radiation. Recently [8] proposed the use of discrete prolate spheroidal (Slepian) sequences as a pulse shaping filter, thus improving the orthogonality of conventional GFDM systems to mitigate self ICI. The performance of these schemes needs to be investigated in multi-input multi-output (MIMO) systems. It is of great interest to exploit the advantages of precoded OSTBC in multicarrier schemes to reduce the effects of inter-antenna interference (IAI) in MIMO scenarios. [9] investigated the application of Alamouti space time coding to mitigate the effects of a multipath environment in such systems. Unlike precoded OSTBC in OFDM systems, the application of such technique is still unexplored in GFDM systems. The objective of this paper is to study symbol error rate (SER) performance of precoded OSTBC under Rayleigh fading channel in both conventional GFDM and Multi-taper GFDM (MGFDM).

The outline of the paper is as follows. In Section II, we give a brief introduction on GFDM, multi-taper implementation to GFDM and precoded OSTBC MGFDM with Alamouti space time coding. In Section III, we provide the analytical performance expressions under the Rayleigh fading channel. Results and conclusions are explained in Section IV. Finally, Section V concludes the paper.

2. System Model

2.1. GFDM Background

GFDM, introduced by [10,11] is a non-orthogonal block based multicarrier technique. Each block consists of KM complex valued data symbols $d_k(m)$ taken from the P-QAM constellation. Each $d_k(m)$ data symbol is distributed across M subsymbols and K subcarriers in time and frequency and modulated by a circular prototype filter $g(n), n = 0, 1, ..., KM - 1$ that provides pulse shaping for each subcarrier according to,

$$g_{k,m}(n) = g[(n - mK) \bmod KM]e^{j2\pi\frac{k}{K}n} \tag{1}$$

where $n = 0, 1, ..., KM - 1$, $g_k(m)$ is the shifted version of the prototype filter $g(n)$ in time (modulo operator) and frequency (complex exponential). The superposition of all the operations leads to the GFDM signal $x(n)$ given by,

$$x(n) = \sum_{k=0}^{K-1}\sum_{m=0}^{M-1} d_k(m)g_{k,m}(n) \quad n = 0, 1, .., KM - 1 \tag{2}$$

In matrix form this can be written as,

$$\mathbf{x} = \mathbf{Ad} \tag{3}$$

where $\mathbf{d}$, the data vector and $\mathbf{A}$, the transmitter modulation matrix are given by [11],

$$\mathbf{d} = [d_0(0), .., d_{K-1}(0), .., d_0(M - 1), .., d_{K-1}(M - 1)]$$

These can also be represented in block structure form according to,

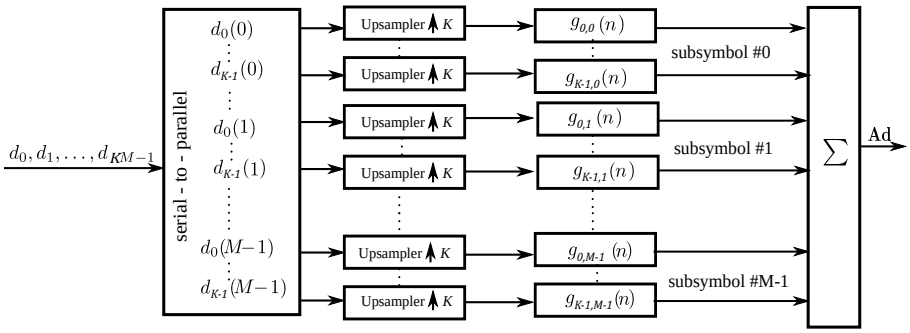

Fig. 1. Details of MGFDM modulator.

$$\mathbf{D} = \begin{pmatrix} d_0(0) & \cdots & d_0(M-1) \\ \vdots & \ddots & \\ d_{K-1}(0) & \cdots & d_{K-1}(M-1) \end{pmatrix} \tag{4}$$

$$\mathbf{A} = [\mathbf{G} \;\; \mathbf{E_1 G} \cdots \mathbf{E_{K-1} G}] \tag{5}$$

where $\mathbf{E_i} = diag\left\{[\mathbf{e_i}^T, ..., \mathbf{e_i}^T]^T\right\}$ is a $KM \times KM$ diagonal matrix whose diagonal elements are comprised of M concatenated copies of the vector $\mathbf{e_i} = [1, e^{j\frac{2\pi i}{K}}, ..., e^{j\frac{2\pi i}{K}(K-1)}]^T$. Matrix $\mathbf{G}$ of size $KM \times M$ is constructed with circular shift of $[g_0, ..., g_{KM-1}]^T$ each of length KM.

2.2. Multi-taper GFDM (MGFDM) Background

In the multi-taper implementation of GFDM introduced by[8], the prototype filter is replaced by the M orthogonal tapers according to,

$$g_{k,m}(n) = g_m(n) e^{\frac{j2\pi kn}{K}}$$

with $g_m(l)$ being the l^{th} coefficient of the mth taper. Asymptotic expressions for the computation of these slepian discrete prolate spheroidal sequences (DPSSs) can be found in[12,13,14]. Some implementation aspects of DPSSs were studied in a recent survey on filters by[15]. In this implementation, the matrix $\mathbf{G}$ of size $KM \times M$ in (5) is constructed by replacing the columns of $\mathbf{G}$ by the first M tapers from the DPSSs. Interestingly, $\mathbf{G}^T\mathbf{G} = \mathbf{I}$, due to taper orthogonality, increases overall system performance in term of error rates compared to conventional GFDM system with the Root Raised Cosine (RRC) filter. Fig. 1 provides the details of MGFDM modulator.

2.3. Precoded OSTBC MGFDM system with Alamouti space time coding

Consider a wireless communication system with N_t transmit antennas and N_r receive antennas whose channel state information (CSI) is assumed to be available at the transmitter. Fig. 2 depicts the proposed block diagram of a feedback precoded OSTBC MIMO-MGFDM system with the Alamouti space coding scheme. In this model, the data vector $\mathbf{d}$ is passed through a space time encoding block to generate the data blocks $\mathbf{D}^1$, $\mathbf{D}^2$ given by (8) according to[16]. A cyclic prefix (CP) is added to both the signals individually as shown in Fig. 2. Note that the length of CP must be larger than the channel impulse response (CIR).

In a precoded OSTBC-MGFDM system, the signal vectors are multiplied by a precoded matrix $\mathbf{W} \epsilon \mathbb{C}^{N_t \times M_c}$, which is selected from the codebook $\mathbf{F} = \{\mathbf{W_1}, \mathbf{W_2}, ..., \mathbf{W_L}\}$, where M_c, L corresponds to codeword length and codebook size respectively. The objective is to choose an optimum codeword which improves the overall system performance in terms of channel capacity or error performance.[17] investigates the criterion for choosing the optimal precoding matrix from the codebook. In brief, the problem for selecting the optimal codeword is directly related to the Grassmannian

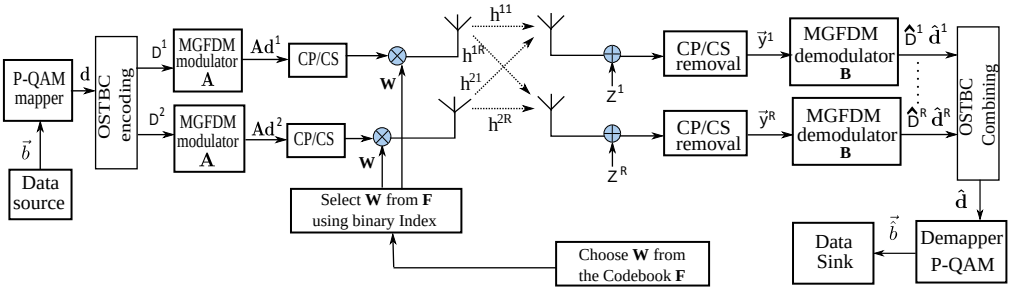

Fig. 2. Block diagram of feedback precoded OSTBC MIMO-MGDFM system with Alamouti space time coding.

subspace packing problem in the Grassmann manifold and proves full diversity order in the Rayleigh fading channel. The optimal codeword can be chosen from the following equation,

$$\mathbf{W_{opt}} = \underset{\mathbf{W}\epsilon\mathbf{F}}{arg\ max} \|\mathbf{hW}\|_F^2 \tag{6}$$

where $\mathbf{h}$ of size $N_r \times N_t$ represents the channel response from transmit antenna N_t to receive antenna N_r and $\mathbf{W_{opt}}$ is the optimal code word chosen from the codebook $\mathbf{F}$.

2.4. Receiver Model

The received signal after the removal of CP can be written as,

$$y^r = \mathbf{h^{1r}Ad^1} + \mathbf{h^{2r}Ad^2} \tag{7}$$

where $\mathbf{h^{tr}} = circ\left\{\mathbf{h_w^{tr}}\right\}$ is the circulant channel matrix and $\mathbf{h_w^{tr}}$ is the multipath channel impulse response (CIR) from transmit antenna t to receive antenna r given by (9) and $\mathbf{h_w^{tr}}$ is zero padded to the length of the transmit signal. $\mathbf{d^t} = vec(\mathbf{D^t})$, where the columns of $\mathbf{D^t}$ are stacked on top of each other[9].

$$\mathbf{D^1} = \mathbf{D},\ \mathbf{D^2} = \left(\begin{array}{cc|cc|c|cc} -d_0^*(1) & d_0^*(0) & -d_0^*(3) & d_0^*(2) & \cdots & -d_0^*(M-1) & d_0^*(M-2) \\ \vdots & \vdots & \vdots & \vdots & \cdots & \vdots & \vdots \\ -d_{K-1}^*(1) & d_{K-1}^*(0) & -d_{K-1}^*(3) & d_{K-1}^*(2) & \cdots & -d_{K-1}^*(M-1) & d_{K-1}^*(M-2) \end{array}\right) \tag{8}$$

$$\mathbf{h_w^{tr}} = \mathbf{hW_{opt}} \tag{9}$$

The signal on each receiver can be demodulated as,

$$\mathbf{d^r} = \mathbf{By^r} \tag{10}$$

The matrix $\mathbf{B} = \mathbf{A}^{-1}$ is the zero forcing receiver matrix. The STC combining is carried according to the following rule[16]:

$$\begin{aligned} \hat{d}_{km} &= \frac{\sum_{r=1}^{R}(H_k^{1r})^* d_{k,m}^r + H_k^{2r}(d_{k,m+1}^r)^*}{\sum_{r=1}^{R}\left|H_k^{1r}\right|^2 + \left|H_k^{2r}\right|^2} \quad m\ even \\ \hat{d}_{km} &= \frac{\sum_{r=1}^{R}(H_k^{1r})^* d_{k,m}^r - H_k^{2r}(d_{k,m-1}^r)^*}{\sum_{r=1}^{R}\left|H_k^{1r}\right|^2 + \left|H_k^{2r}\right|^2} \quad m\ odd \end{aligned} \tag{11}$$

where H_k^{tr} denotes the kth point DFT of the CIR $\mathbf{h_w^{tr}}$.

Table 1. Simulation Parameters

Description	GFDM	GFDM-DPSS
Number of Subcarriers, K	64	64
Number of time slots, M	8	8
Pulse shape filter, g	RRC	DPSS
Roll-off factor, α	{0.1}	-
Length of CP, N_{cp}	10	10
Modulation order, μ	4	4
(N_t, N_r)	(2,1)	(2,1)

3. Performance Analysis

In this section we provide the symbol error rate (SER) theoretical expressions for the precoded OSTBC GFDM system under consideration by using the upper bound probability for the maximum ratio combiner[1]. Note that the effect of the noise enhancement factor (NEF) and the precoding matrix is taken into account and the approximate expression is given by,

$$P_e = 4\eta \sum_{i=0}^{N_t N_r - 1} \binom{N_t N_r - 1 + i}{i} \left(\frac{1+\lambda}{2}\right)^i \tag{12}$$

where

$$\eta = \left(\frac{\sqrt{P}-1}{\sqrt{P}}\right)\left(\frac{1-\lambda}{2}\right)^{N_t N_r}$$

$$\lambda = \sqrt{\frac{\frac{3\left\|\mathbf{h^{tr}}\right\|_F^2}{2(P-1)}\frac{E_s}{N_0 R N_t \xi_0}}{1+\frac{3\left\|\mathbf{h^{tr}}\right\|_F^2}{2(P-1)}\frac{E_s}{N_0 R N_t \xi_0}}}$$

$$\xi_{0,GFDM} = \xi \frac{KM + N_{cp} + N_{cs}}{KM}$$

R, the symbol rate of the OSTBC is given by $R = \frac{Q}{T}$ where T time periods are used to transmit Q symbols. NEF ξ under a GFDM system with zero forcing receiver is given by,

$$\xi = \sum_{n=0}^{KM-1} \left|[\mathbf{B}]_{k,n}\right|^2 \tag{13}$$

The values of ξ are equal for any index k. Under an MGFDM system, NEF is given by[8]

$$\xi = min\left\{\sum_{n=0}^{KM-1} \left|[\mathbf{B}]_{k,n}\right|^2\right\} = 1 \tag{14}$$

4. Results and Discussions

In this section we present the simulation results to illustrate and verify the SER of STBC-MGFDM, precoded OSTBC MGFDM and precoded OSTBC-GFDM under the Rayleigh fading channel. The simulation parameters under consideration are mentioned in Table 1. Furthermore, the code book generation for a different number of antennas are mentioned in Table 2. Throughout the simulation we have considered 16-QAM, $N_t = 2$ and $N_r = 1$.

Fig. 3 illustrates the SER performance comparison for both STBC-MGFDM and precoded OSTBC MGFDM systems. The solid or dashed lines correspond to the theoretical expressions (12) and (14) while the labels correspond to simulations. It can be observed that there is an improvement in performance with precoded OSTBC (curves (i)–(ii)).

Table 2. Codebook design parameters for OSTBC in IEEE 802.16e

N_t	Codeword length, M_c	Codebook size, L	Rotation Vector , **u**
2	1	8	[1,0]
3	1	32	[1,26,28]
4	2	32	[1,26,28]
4	1	64	[1,8,61,45]
4	2	64	[1,7,52,56]
4	3	64	[1,8,61,45]

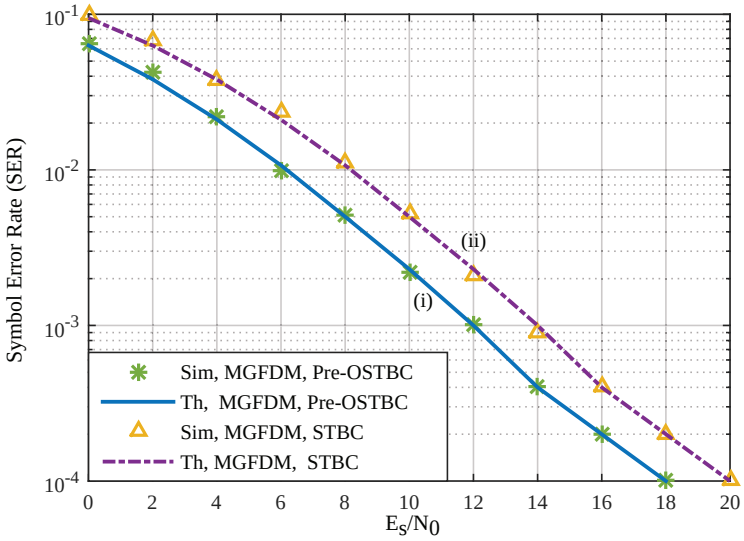

Fig. 3. Comparison plot for precoded OSTBC MGFDM and STBC MGFDM systems with 16-QAM, Rayleigh fading channel.

For example at an SER of 10^{-4} there is an additional 2dB required for STBC-MGFDM compared to the precoded OSTBC-MGFDM.

Fig. 4 demonstrates the SER performance for precoded OSTBC under both MGFDM and conventional GFDM with roll-off factor $\alpha = 0.1$ using 16-QAM over a flat Rayleigh fading channel. With the use of prolate windows we can compensate the orthogonality loss in conventional GFDM systems and as is evident from the figure, the same holds with the application of precoded OSTBC. There is a good match between the derived analytical expressions and the simulated results. An SER of 10^{-3} is achieved at an E_s/N_0 of approximately 12dB for the precoded OSTBC-MGFDM system ((curve (i)) and 17dB in the case of the precoded OSTBC-GFDM system (curve ((ii)).

5. Conclusion

In this paper, we investigated the performance of conventional GFDM and MGFDM systems combining the Alamouti scheme and precoded OSTBC over a Rayleigh fading channel. More explicitly, we derived analytical SER expressions of precoded OSTBC-MGFDM and conventional GFDM systems. The derived analytical results are then validated through simulations. Our analysis proves that there is an improvement in SER performance when comparing STBC-GFDM systems to conventional GFDM as well as a higher diversity advantage. In fact, with the further use of multi-tapers as prototype filters we observe a still additional improvement in an OSTBC-GFDM system. To conclude, the implementation of precoded OSTBC in GFDM systems is beneficial and provides robustness to the overall system performance. Further investigations can be carried out for a variety of other modulation schemes, multi-path and fading conditions and that is the focus of our future work.

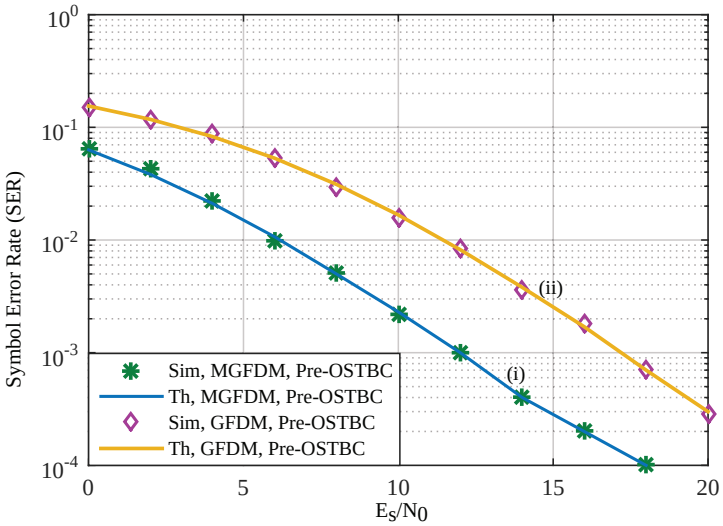

Fig. 4. Comparison plot under precoded OSTBC technique for both MGFDM and conventional GFDM systems with 16-QAM.

References

1. Tse, D., Viswanath, P.. *Fundamentals of wireless communication*. Cambridge university press; 2005.
2. Alamouti, S.M.. A simple transmit diversity technique for wireless communications. *Selected Areas in Communications, IEEE Journal on* 1998;**16**(8):1451–1458.
3. Tarokh, V., Jafarkhani, H., Calderbank, A.R.. Space-time block codes from orthogonal designs. *Information Theory, IEEE Transactions on* 1999;**45**(5):1456–1467.
4. Jöngren, G., Skoglund, M., Ottersten, B.. Combining beamforming and orthogonal space-time block coding. *Information Theory, IEEE Transactions on* 2002;**48**(3):611–627.
5. Jöngren, G., Skoglund, M.. Improving orthogonal space-time block codes by utilizing quantized feedback information. In: *2001 IEEE International Symposium on Information Theory (ISIT 2001); Washington, DC*. IEEE; 2001, p. 220.
6. Wang, H., Li, Y., Xia, X.G., Liu, S.. Unitary and non-unitary precoders for a limited feedback precoded ostbc system. *Vehicular Technology, IEEE Transactions on* 2013;**62**(4):1646–1654.
7. Hjørungnes, A., Gesbert, D.. Precoded orthogonal space–time block codes over correlated ricean mimo channels. *Signal Processing, IEEE Transactions on* 2007;**55**(2):779–783.
8. authors previous work submission, . Multi-taper implementation of gfdm. In: *IEEE Wireless Communications and Networking Conference 2016; Accepted for publication*. 2016, .
9. Matthé, M., Mendes, L.L., Fettweis, G.. Space-time coding for generalized frequency division multiplexing. In: *European Wireless 2014; 20th European Wireless Conference; Proceedings of*. VDE; 2014, p. 1–5.
10. Fettweis, G., Krondorf, M., Bittner, S.. Gfdm-generalized frequency division multiplexing. In: *Vehicular Technology Conference, 2009. VTC Spring 2009. IEEE 69th*. IEEE; 2009, p. 1–4.
11. Michailow, N., Matthé, M., Gaspar, I.S., Caldevilla, A.N., Mendes, L.L., Festag, A., et al. Generalized frequency division multiplexing for 5th generation cellular networks. *Communications, IEEE Transactions on* 2014;**62**(9):3045–3061.
12. Slepian, D.. Prolate spheroidal wave functions, Fourier analysis, and uncertainty-V: The discrete case. *Bell System Technical Journal* 1978; **57**(5):1371–1430.
13. Slepian, D.. Some asymptotic expansions for prolate spheroidal wave functions. *J Math Phys* 1965;**44**(2):99–140.
14. Thomson, D.J.. Spectrum estimation and harmonic analysis. *Proceedings of the IEEE* 1982;**70**(9):1055–1096.
15. Sahin, A., Guvenc, I., Arslan, H.. A survey on multicarrier communications: Prototype filters, lattice structures, and implementation aspects. *Communications Surveys Tutorials, IEEE* 2014;**16**(3):1312–1338.
16. Matthé, M., Mendes, L.L., Fettweis, G.. Space-time coding for generalized frequency division multiplexing. In: *European Wireless 2014; 20th European Wireless Conference; Proceedings of*. VDE; 2014, p. 1–5.
17. Love, D.J., Heath Jr, R.W.. Limited feedback unitary precoding for orthogonal space-time block codes. *Signal Processing, IEEE Transactions on* 2005;**53**(1):64–73.